Molecular Crystals and Liquid Crystals Science and Technology. Section A. Molecular Crystals and Liquid Crystals

Publication details, including instructions for authors and subscription information:
http://www.tandfonline.com/loi/gmcl19

Textures in 2D-Confined Circular Domains on a Polar Smectic Film

Isabelle Kraus [a] & Robert B. Meyer [b]

[a] Institut de Physique et Chimie des Matériaux, Groupe des Matériaux Organiques, 23 rue du Loess, F-67037, Strasbourg, France

[b] The Martin Fisher School of Physics, Brandeis University, Waltham, MA, 02254-9110, U.S.A.

Version of record first published: 24 Sep 2006

To cite this article: Isabelle Kraus & Robert B. Meyer (1999): Textures in 2D-Confined Circular Domains on a Polar Smectic Film, Molecular Crystals and Liquid Crystals Science and Technology. Section A. Molecular Crystals and Liquid Crystals, 328:1, 523-531

To link to this article: http://dx.doi.org/10.1080/10587259908026096

Mol. Cryst. Liq. Cryst., 1999, Vol. 328, pp. 523-531
Reprints available directly from the publisher
Photocopying permitted by license only

Textures in 2D-Confined Circular Domains on a Polar Smectic Film

ISABELLE KRAUS[a] and ROBERT B. MEYER[b]

[a]*Institut de Physique et Chimie des Matériaux, Groupe des Matériaux Organiques, 23 rue du Loess, F-67037 Strasbourg, France; and* [b]*The Martin Fisher School of Physics, Brandeis University, Waltham, MA 02254–9110, U.S.A.*

We observe textures on polar smectic films, using a new approach to achieve the polar geometry. We concentrate on 2D confined circular domains, for which we observed a "boojum" pattern and a previously unobserved spiral texture that reverses it direction of winding at a critical radius. The mapping of the c-vector is given in each case. The textures are understood in light of a free energy with one additional K_{sb} bulk term and one additional λ_s boundary term.

Keywords: pattern; texture; smectic; polar film; free standing film; boojum; spiral

INTRODUCTION

Polar smectic films consist of well ordered molecular layers, arranged parallel to the plane of the film, with one interface in contact with air and the other one in contact with liquid. Due to the drastic change in the local surrounding of the molecules placed at the interfaces, there is a surface polarization at each film limit. These two surface polarizations do not cancel because of the different nature of the two interfaces involved, leading to a net polarity over

the whole thickness of the film. Among examples of polar smectic films are wetting films induced on top of a mesogenic drop[1], or Langmuir films[2] consisting, e.g., of fatty acid put at the interface between water and air. In this paper, we concentrate on some patterns observed in circular domains of constant thickness on polar smectic films. The study is held under different film thickness in order to examine the consequences of the breaking of the film planar symmetry on the textures.

EXPERIMENTAL SET-UP:

To achieve polar geometry, we develop a new technique[3]. A smectic film with two free surfaces in contact with air is drawn on a circular metallic frame about 6mm in diameter. Using a micrometer screw, the film is lowered toward a liquid drop deposited on a treated glass plate, up to the point where there is contact. The polar film is formed on top of the drop and it is delimited by a meniscus which is an excess of compound. The polar film is still in contact with the frame via the remaining of the free standing (FS) film. This allows us to vary the polar film area by adjusting the vertical position of the film holder.

With this procedure, the molecular arrangement in a circular domain can be studied first within a non-polar configuration, the FS film, then, within a polar configuration when the film is put on the liquid drop. Moreover, we can tune-up the strength of the polar effect using the fact that the thickness of the initial FS film can be varied from 2 to thousands layers: Thicker is the sample, less influence has the surface layers over the whole thickness of the film.

The images presented in the paper are obtained using a commercial compound, Chisso CS1015, having a fairly large chiral SmC* temperature range around room temperature. Its phase sequence is: K– (-17°C) –SmC*–

(57°C) –SmA– (68°C) –N– (78°C) –I. The samples are deposited on distilled water and observed between crossed polarizers using a light transmission microscope. This way, the spatial variation of the c-vector, the projection of the molecular long axis on the plane (x,y) of the film, can be detected. In order to have more light intensity going through the sample, the polarizer-analyzer are slightly uncrossed so that two consecutive gray areas on Fig. 1b and 1c correspond to a c-vector rotation of a factor of π and not $\pi/2$, like on Fig. 1a. The experiment is run at 20°C to limit the evaporation of the wetting liquid.

OBSERVATIONS

The main characteristics of the polar films obtained using our technique are discussed elsewhere[3]. The observation of rapid fluctuations of the c-vector in all studied cases, convinced us that the samples were in the SmC* phase.

Textures seen in domains are the result of a topological constraint and of an energetical constraint. The circular topology of the domain together with the strong anchoring of the c-vector on its limit, impose the presence of a point singularity around which the c-vector rotates once. Its position as well as the c-distribution within the domain is given by the energetic of the system.

In the case of an air/air interface free standing film, the point defect is generally located at about the middle of the drop and it corresponds to the center of a pure bend distortion of the c-distribution[4]. The radial configuration, with planar anchoring of the c-vector at the edge, leads to a cross-shaped pattern shown on Fig. 1a. This configuration minimizes the free energy when the Frank elastic constant for bend is lower than that for splay[5].

Lowering the symmetry of the system by putting it onto water, and looking at films tens layers thick, we observe that the point defect is no more at the middle of the domain but it has been "expelled" from the center to the edge (Fig. 1b). Straight schlieren lines that correspond to loci of constant orientation of the c-vector, emerge from the defect up to the edge, meeting the lateral boundary at an angle with respect to the direction of the polarizers, positioned along the frame of Fig. 1b. This indicates that we do not have anymore tangent anchoring at the boundary but oblique anchoring of the c-vector along the edge. This pattern is known as the "boojum" texture.

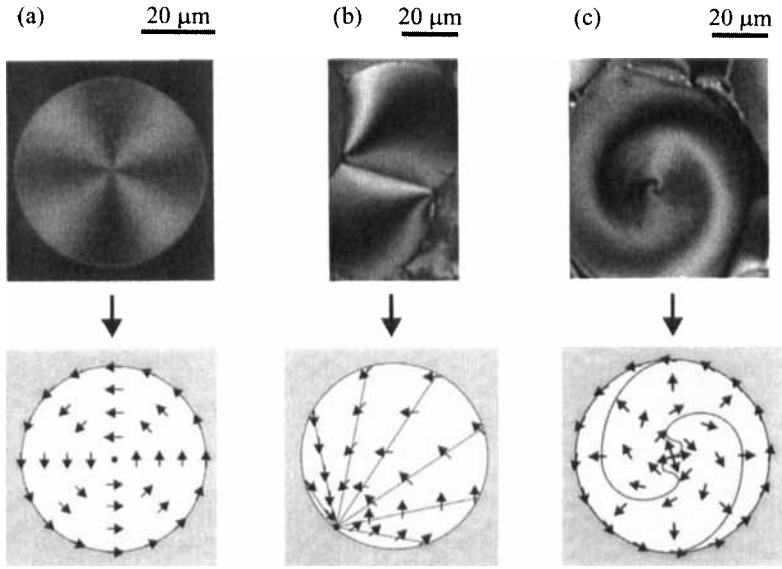

FIGURE 1 Patterns observed in circular domains on a regular free standing film (a), and on a polar smectic film: the boojum pattern (b) and the reserving spiral pattern (c).

Contrary to the similar textures observed in isolated domains of Langmuir films[6] (LM) or in SmI domains nucleated into a SmC free standing film[7] (I/C) where a "virtual" topological defect is located outside the domain, the point singularity on Fig. 1b appears to be right at the edge, at least to optical resolution. It emphasizes that the boundary anchoring of the c-vector in our polar films is stronger relative to the defect energy. We speculate that this strong anchoring results from the large change in layer thickness associated with the domain limit in our case, compared to the relatively weak changes in molecular configuration associated with the phase boundary that defines domains in LM and I/C systems.

Looking at thicker polar films, i.e., lowering the effect of the polar geometry, we observed another type of texture presented on Fig. 1c. The point singularity, located at the center of the domain, is the starting point of a spiral that begins to wind counter-clockwise and at a critical radius reverses its winding direction before meeting the edge of the domain. We call this pattern the "reversing spiral". The c-distribution is purely radial. Following the c-vector along a radius (see Fig. 2), and starting at the defect with an angle $\phi_d \approx 0$ between the c-vector and the radial direction, we continuously rotate up to a value close to $-\pi/2$, reached at the critical radius, and then rotate back to match the value $\phi_b \approx +\pi/2$ on the edge. The critical radius is estimated to be about $r_o/3$.

THEORITICAL DEVELOPMENT

To understand the patterns observed, we consider a 2D smectic model, making the assumption that the tilt angle of the molecules with respect to the normal to the film surface is a constant throughout the sample. The

justification of this simplification is discussed elsewhere[3]. We will also consider chiral molecules.

Following Langer and Sethna[7], the elastic free energy for the c-vector in a circular domain of a chiral polar SmC* thin film can be written as:

$$F = \int_{Area} dA \left[K_s (\nabla \cdot \hat{c})^2 + K_{sb} (\nabla \cdot \hat{c}) \{ (\nabla \times \hat{c}) \cdot \hat{z} \} + K_b \{ (\nabla \times \hat{c}) \cdot \hat{z} \}^2 \right] \oint_{Boundary} dl \left[\lambda_s (\hat{c} \cdot \hat{m}) + \lambda_b \{ (\hat{c} \times \hat{m}) \cdot \hat{z} \} \right] \quad (1)$$

where K_s and K_b are the splay and bend curvature constants, λ_s and λ_b give the strength of the lowest order terms dictating the c-vector anchoring at the domain limit, $\hat{m}$ is the outward normal to the boundary, and $\hat{z}$ is the normal to the film plane. We require that K_s and K_b be positive and that $K_{sb}^2 < 4K_sK_b$ to make F positive definite for arbitrary values of splay and bend.

Compared to the corresponding free energy expression written for a regular free standing film, the K_{sb} and λ_s terms are new. They are allowed in the F-expression because the polar system is no more invariant under rotation around the 2-fold axes about x and y. The presence of these two additional terms is crucial to understand the observed textures: The K_{sb} term implies that the minimum energy of the system is no more a pure splay or a pure bend configuration of the c-vector, but a unique combination of splay and bend; the λ_s term, together with the λ_b term allow oblique anchoring of the c-vector along the edge.

DISCUSSION

Considering the boojum pattern, the presence of oblique anchoring revealed on Fig. 1b leads to a non zero contribution of the K_{sb} bulk term in Eq. (1). In terms of the polar coordinates (r,θ) centered on the point defect, and of ϕ the c-vector angle relative to the radial vector, a stable solution of the Euler-Lagrange equation is $\phi = \theta + \phi_b$, independent of r. This solution, in a circular domain of radius r_o centered at the point $(r_o, 0)$ has the fixed angle ϕ_b between $\hat{c}$ and $\hat{m}$ at all points on the domain edge.

In the case of the reversing spiral pattern, the c-distribution is a function of the polar coordinate r, only. Making the transformation $x = \ln(r/\varepsilon)$ where ε is the defect core radius, the Euler-Lagrange equation has a first-integral, which leads to:

$$\left(\frac{d\phi}{dx}\right)^2 = \frac{Q + B(\phi)}{A(\phi)} \tag{2}$$

with:

$$B(\phi) = 1 + \beta\cos(2\phi) + \Gamma\sin(2\phi)$$
$$A(\phi) = 1 - \beta\cos(2\phi) - \Gamma\sin(2\phi)$$

Q is a constant of integration, $\beta = \frac{K_s - K_b}{K_s + K_b}$, and $\Gamma = \frac{K_{sb}}{K_s + K_b}$. The constant Γ is directly linked to the polar geometry of our system. Equation (2) is similar to the Euler-Lagrange solution for a Freedericks transition in nematic[8], provided the effective uniform magnetic field term is given by:

$$B(\phi) = -\chi_a\left(\vec{H}_{eff}\cdot\hat{c}\right)^2.$$

We extract an angle α between the effective field and the radial direction, given by the relation $\Gamma/\beta = \tan(2\alpha)$. Thus, the reversing spiral pattern will be

the result of a competition between the favored direction imposed by $\vec{H}_{eff}$ in the bulk and the strong anchoring conditions at both limits, the defect and the edge, as for the Freedericks transition. This remark is illustrated on Fig. 2, taking the c-distribution scheme for the reversing spiral (Fig. 1c) and unwinding the circular domain to make it a strip of SmC* contained between two parallel lines at which the boundary conditions on ϕ are ϕ_d at the defect and ϕ_b at the edge, with an applied magnetic field at angle α.

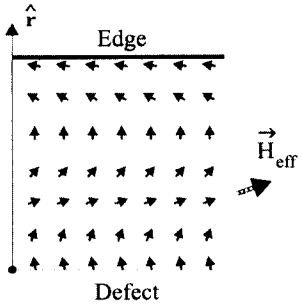

Figure 2 Radial c-distribution of Fig. 1c reversing spiral.

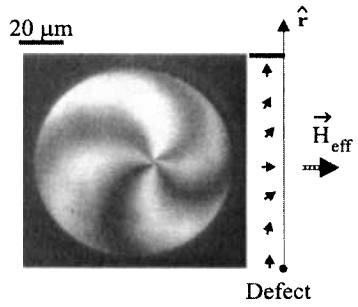

Figure 3 Reversing spiral seen on a free standing film.

Let us underline that the B(ϕ)-term exists also for Γ equals to zero, i.e., for a free standing film. Indeed, going back to experiments on the non-polar films, we see reversing spirals in domains with radius superior to 30 μm, as shown on Fig. 3. The critical radius for which the spiral reverses its direction of winding is much smaller than on a polar film, so that the spiral reverses

closer to the defect point and it is harder to detect and not as beautiful to observe. The competition happens now between the bulk, which favors pure bend, and the boundary that favors radial anchoring at the defect and along the edge.

The next step will be to introduce a thickness dependence in the free energy considering a tilt angle of the molecules that varies continuously along z. But already using the development of Eq. (1), we were able to explain the main features of our observations.

Acknowledgments

We thank Jay Patel, Darren Link and Noel Clark for providing us with chemical compounds. I.K. is grateful to the city of Strasbourg for financial support through a Strasbourg-Boston twin cities fellowship. This research was supported by the NSF through grant DMR-9415656 and by the Martin Fisher School of Physics at Brandeis Universtity.

References

[1] R. Luth, Ch. Bahr, G. Heppke, J.W. Goodby, J. Chem. Phys. **108**, 3716 (1998); V. Candel, Y. Galerne, Phys. Rev. Lett. **70**, 4083 (1993).
[2] B. Rapp, H. Gruler, Phys. Rev. A **42**, 2215 (1990); C.M. Knobler, Physica A **236**, 11 (1997) and references therein.
[3] I. Kraus, R.B. Meyer, to be published.
[4] J.E. Maclennan, U. Sohling, N.A. Clark, M. Seul, Phys. Rev. E **49**, 3207 (1996), section IV.B.
[5] C. Rosenblatt, R. Pindak, N.A. Clark, R.B. Meyer, Phys. Rev. Lett. **42**, 12 (1979).
[6] S. Riviere, J. Meunier, Phys. Rev. Lett. **74**, 2495 (1995).
[7] S.A. Langer, J.P. Sethna, Phys. Rev. A **34**, 5035 (1986).
[8] P.G. de Gennes, J. Prost, *The Physics of Liquid Crystals,* 2nd edn. (Clarendon Press, Oxford, 1993).